Dolomite study for in-situ CO_2 capture for chemical looping reforming

P. Pimenidou[a,*], V. Dupont[b]

a Built Environment Institute, University of Ulster, Newtownabbey, BT37 0QB, UK

b Energy and Resources Institute, The University of Leeds, Leeds, LS2 9JT, UK

*Corresponding author. Email: p.pimenidou@ulster.ac.uk

Dolomite study for in-situ CO_2 capture for chemical looping reforming

The non- isothermal kinetic and thermal behaviour of a naturally formed dolomite in conditions that approach in-situ CO_2 capture in chemical looping reforming, chiefly the use of the packed bed configuration, were investigated. The performance of this dolomite was studied at micro-scale in 'dry' conditions, as well as at macro-scale in 'dry' and 'wet' conditions to investigate the effects of scale (3mg, 2.5g), partial pressures of CO_2 (<15kPa) and steam, and deactivation upon limited cycling. The carbonation and calcination kinetics were modelled using an improved iterative Coats-Redfern method. Increasing CO_2 partial pressures on the 'dry' macro-scale exacerbated the experimental carbonation conversions in an inversely proportional trend when compared to those at micro-scale. The presence of steam had a positive effect on CO_2 chemisorption. Steam had a negligible influence on the calcination activation energies. The activation energies of carbonation were increased for the experiments at the highest CO_2 partial pressures under wet conditions.

Keywords: dolomite, CO_2 capture, kinetics, modelling, steam

1. Introduction

At present, there is an intense interest in chemical looping systems (Blamey *et al.* 2010, Li *et al.* 2008) which have so far been mainly developed for the combustion industry and applied to fluidized bed technology (Chen *et al.* 2011, Sun *et al.* 2008). Lyon and Cole (2000) suggested unmixed combustion which has been lately deployed in the chemical looping technology (Dupont *et al.* 2007, Pimenidou *et al.* 2010a). Furthermore, the reduction of CO_2 emissions is a topic of particular priority in the framework of sustainable energy and low-carbon energy technologies as well as a key issue in today's agenda of most of the developed countries. By incorporating simultaneously the chemical looping reforming and ('in- situ') CO_2 capture (Curran *et al.* 1967, Pimenidou *et al.* 2010b, Giannakeas *et al.* 2012), a high purity H_2 product emerges, without any further separation of unwanted product gases, for direct utilisation i.e. in fuel cells. Calcium looping particularly proved to be the cheapest option for CO_2 capture (Romeo *et al.* 2009) based on CO_2 avoided cost (Abanades *et al.* 2007).

Moreover, materials are sought for CO_2 capture, which will reduce the energy consumption by increasing the production efficiency of the energy carriers. There is a great variety of synthetic CO_2 capture materials currently applied, such as zeolites (e.g. NaX, 5A), which pose some difficulty in adsorbing H_2O when used to capture CO_2 from gases. Most of synthetic materials are costly to produce (such as zeolites for physisorption and MEA (Monothanolamine)) when their application is energy consuming (Rao and Rubin 2006). Dolomite and dolomite based sorbents offer smaller efficiency penalties than amine- based post- combustion capture. Calcium oxide (CaO) used for CO_2 capture was first mentioned by DuMotay and Marechal in 1867 who enhanced the gasification of carbon by steam with lime (Barker 1973). The suitability of metal oxides (Me_xO_y) in capturing CO_2 at temperatures

between 550°C and 750°C at atmospheric pressure (101.3 kPa) has been demonstrated in the past six decades (Pimenidou *et al.* 2010b, Hyatt *et al.* 1958, Squires 1967, Dou *et al.* 2010).

The key reaction for the capture of CO_2 by CaO is the following,

$$CaO + CO_2 \rightarrow CaCO_3$$

which is considered in post- combustion or in-situ capture of CO_2 processes as well as in energy storage (Aihara *et al.* 2001) with further encounter in flue gas CO_2 separation (Han and Harrison 1994) and hydrocarbon and water gasification for H_2 production (Gupta and Fan 2002). The exothermicity of this reaction has also proven to offer autothermal intervals during in- situ use in chemical looping steam reforming for hydrogen production (Pimenidou *et al.* 2010b).

Calcium oxide may be formed from the thermal decomposition (calcination) of dolomite, which when in a CO_2 environment takes place in two stages (Gupta and Fan 2002, McIntosh *et al.* 1990, Chrissafis *et al.* 2005a, Chrissafis *et al.* 2005b):

$$MgCa(CO_3)_{2(s)} \rightarrow MgO_{(s)} + CaCO_{3(s)} + CO_{2(g)} \quad \text{(TDa)}$$

$$CaCO_{3(s)} \rightarrow CaO_{(s)} + CO_{2(g)} \quad \text{(TDb)}$$

MgO gives stability in the sorbent's structure which in the long term gives more durability to this material compared to limestone (Gupta and Fan 2002). The thermal decomposition reaction of $MgCa(CO_3)_{2(s)}$ may occur in a single step (McIntosh *et al.* 1990, Samtani *et al.* 2002) in an inert environment as in pure gaseous nitrogen (N_2),

$$MgCa(CO_3)_{2(s)} \rightarrow MgO_{(s)} + CaO_{(s)} + 2CO_{2(g)} \quad \text{(TD)}$$

This step regenerates the 'in- situ' adsorptive material in chemical looping steam reforming like in the exothermic oxidation step of air feed over the reduced Ni- based

catalysts (Dupont *et al.* 1997, Pimenidou *et al.* 2010a, Giannakeas *et al.* 2012, Dou *et al.* 2010). The reversibility of calcination has been confirmed by numerous investigators (Barker 1973, Chrissafis *et al.* 2005b).

Calcined dolomite fulfils the requirements of high carbonation capacity and low cost. When CaO is combined with a metal catalyst in chemical looping reforming, catalyst deactivation is prevented and unfavourable fuels conversion in a rich H_2 syngas is enhanced (Giannakeas *et al.* 2012). However, its stability under repeated calcinations/ carbonation cycles has often been rated as poor mostly based on microbalance and TGA studies ('micro-scale') (Chrissafis *et al.* 2005a), despite exhibiting a higher stability than limestone (Abanades and Alvarez 2003).

The kinetics of the calcination- carbonation reactions were sparsely studied, by L'vov and Ugolkov (2003), Olszak- Humienik and Możejko (1999), Samtani *et al.* (2002) with regard to the calcinations and by Lee (2004) with regard to the carbonation reaction.

The effect of steam and CO_2 on these metal oxides was investigated in the high CO_2 pressure regime of the reaction (TDa) by Beruto *et al.* (2003). The effect of steam in the DTA analysis of $CaCO_3$ decomposition in nitrogen as well as in the carbon dioxide atmosphere found in calcite and dolomite was previously examined by McIntosh *et al.* (1990). Ochoa-Fernandez *et al.* (2007) posited that the increase in the kinetics and the carbonation capacity of synthetic ceramic CO_2 sorbents (Li_2ZrO_2 and Na_2ZrO_2) due to the presence of steam was accredited to the increased ion mobility. Hydrotalcites have been reported to be ill-influenced by the presence of steam (Ficicilar and Dogu 2006, Ding and Alpay 2000). The effect of steam which enhances the kinetics of carbonation of Ca based sorbents is a known but poorly quantified phenomenon, and is generally attributed to the increased CO_3^{2-} ions transport in a steam environment.

In chemical looping reforming, the sorbent needs to exhibit fast kinetics during the CO_2 adsorption at low CO_2 partial pressures, while stability is maintained and capacity is regained. Operating under such conditions creates specific environments for the carbonation and the thermal decomposition of the sorbent. The morphology of CO_2 sorbents should be characterized by large pores with small particles and a large surface area in order to guarantee a long- lasting and efficient performance while sintering is minimized.

This study is focused on the kinetic and thermal study of naturally formed dolomite under conditions which assimilate chemical looping reforming at atmospheric pressure, offering the isolation of the adsorption and regeneration reactions mentioned earlier. These environments of in- situ CO_2 capture, chiefly the use of the packed bed configuration, low CO_2 partial pressure and the presence of steam are investigated and the produced apparent kinetic parameters are also discussed in order to determine optimum conditions of the in- situ employment of naturally formed dolomite in chemical looping reforming. Non- isothermal experiments were performed in a TGA (few milligrams; micro- scale) and lab reactor (few grams; macro- scale) in the absence ('dry' experiments) and in the presence ('wet' experiments) of steam.

2. Experimental and numerical section

2.1 Experimental section

Material: Natural dolomite was obtained through WBB Minerals (Warmsworth quarry, West Yorkshire, UK) as a graded aggregate in a fully carbonated form. The chemical analysis of the calcined dolomite, supplied as information data sheet, showed that its composition on a mass basis was: 30.70% CaO, 21.30% MgO, 0.30% SiO_2, 0.27% Fe_2O_3, 0.10% Al_2O_3 and 47.34% CO_2. Particles of 1- 1.4 mm size were used in micro- and macro- scale experiments

after manually grinding and sieving (BS410) the as received dolomite. Natural dolomite from Spain of 1- 2 mm particles had been earlier used in packed bed reactor for chemical looping reforming (Dupont *et al.* 2007). For the kinetics study at micro- scale and for the thermal stability study 3 and 10 mg of these particles were used respectively, whereas for the investigation at macro- scale, 2.5 g of the same size 'fresh' (fully carbonated) dolomite particles were used.

Micro- scale (Thermogravimetric analysis (TGA)) set- up: A thermogravimetric analyzer (Shimadzu TGA-50) was used. Any changes in the weight of the sample were measured and recorded with the TA 60 data collection software while it was heated up at 10 ^{o}C min^{-1} or cooled down with a cooling blower. Three heating/ cooling cycles were carried out for the kinetic study, at several pressures of gaseous CO_2 (P_{CO_2}= 5- 15 kPa) at 100 kPa N_2. The required mass flow rate of each gas in the TGA was controlled by an MKS Instrument Type 247C four channel readout controller and verified by using a CSI 6000 Solid State calibration flow meter. The gas mixture flow rate was set at 50 cm^3 min^{-1} (STP). The same heating rate and experimental set- up was also used in the thermal stability study only that an initial mass of 10 mg and a 10 kPa CO_2 pressure was used for both calcination/ carbonation steps.

Macro- scale set-up: The set- up of these experiments was performed in a reactor rig as in Pimenidou *et al.* (2010a). The sorbent samples were sandwiched between beds of alumina oxide granules (4-8 mesh; SIGMA ALDRICH). Macro- scale calcination and carbonation runs occurred at a heating rate of 10 ^{o}C min^{-1} (up to 800 ^{o}C) as in the micro-scale experiments. The linearity of the temperature increase in the reactor was verified in the dolomite bed. Temperatures were monitored by 3 thermocouples (Type K) inserted in the sorbent bed; one at the top surface, one in the middle of the sorbent bed and the third one at the bottom surface of the bed. The gases flowed from the bottom end of the reactor and left at

the top end. In both 'dry' and 'wet' experiments the flow rate of N_2 was 750 cm^3 min^{-1} (STP), with the CO_2 flow added to it for the carbonation runs resulting in pressures of 5, 10 and 15 kPa CO_2 (P_{CO_2}). Similarly to the micro- scale experiments, the maximum volume of CO_2 which would be required for the full carbonation of the maximum theoretical CaO moles from the fully calcined 2.5 g of the fresh sorbent ($MgCa(CO_3)_2$) was calculated in order to ensure the reactant gas was in excess. This CO_2 volumetric flow rate corresponds to the following molar flow rate,

$$\dot{n}_{CO2} = \frac{P\dot{V}_{CO_2}}{RT} = \frac{(101.325\ kPa) \times (0.05\ L\ min^{-1})}{(8.314\ L\ kPa\ K^{-1}\ mol^{-1}\ 293K)} = 0.021\ moles\ min^{-1}$$

which is sufficient for the $n_{\max\ (CaO)}$= 0.0137 moles. For the 'wet' experiments, deionised water was pumped in a pre-heater situated beneath the reactor and was evaporated at 200°C; the temperature of the reactor was also at 200°C when the steam was initially supplied. During the 'wet' runs, the liquid flow rates of deionised water used were: 0.017, 0.045 and 0.073 cm^3 min^{-1} for the 5, 10 and 15 kPa CO_2 pressures. This resulted in H_2O vapor partial pressures of 2.8, 6.8 and 10.1 kPa (P_{H_2O}). Steam leaving the reactor was condensed and any left- over moisture was trapped downstream of the condenser using a silica gel trap. A second silica gel trap was used just upstream of the analyzer in order to avoid moisture entering it.

CO_2 content in the effluent gases was monitored online by an NDIR absorption gas analyzer (Uras 14, ABB), connected to a display and control unit. The smallest measurement range for CO_2 was 0-100 ppm. Similarly to the micro- scale thermal stability study, the 'dry' and 'wet' macro- scale tests were performed for both calcination and carbonation steps at 10 kPa CO_2 during heating at a rate of 10 ^oC min^{-1}. All experiments were conducted at atmospheric pressure in order to avoid resistance of external mass transfer.

2.2 Numerical

2.2.1 Micro- scale calculations

Conversions of the reactants in the calcination and carbonation reactions under all conditions were calculated based on the absolute CO_2 capacity of the employed mass of sorbent. The final conversion of the reactants, for both calcination/ carbonation reactions, is defined by:

$$a^i(\%) = \frac{M^o}{W_{CO_2}} \cdot \frac{(P^i_{sorb} - P^{f,i-1}_{sorb})}{N^{f,i-1}_{sorb}} \qquad (1)$$

$$\text{where } P^i_{sorb} = 100 \times \frac{M^i_{sorb}}{M^{f,i-1}_{sorb}} \qquad (2)$$

P_{sorb} is the percentage mass of the sorbent (oxide + carbonate; $CaO.CaCO_3$) remaining in the TGA crucible at any time during a specific step of the experiment of index 'i'. M^o is the initial mass of 'fresh' dolomite in the TGA crucible while M^i_{sorb} is the mass of sorbent remaining in the TGA at any time during the experiment of index 'i'. The integer superscripts i-1 and i indicate preceding and present runs (steps) respectively.

By the end of the thermal decomposition the final molecules of $CaCO_3$ ($N^{f,i}_{CaCO_3}$) and CaO ($N^{f,o}_{CaO}$) in the sample were calculated by equations 3 and 4, when $(-1)^i < 0$,

$$N^{f,i}_{CaCO_3} = \left(1 - \frac{\alpha^{f,i}}{100}\right) . N^{f,i-1}_{CaCO_3} \quad (3)$$

$$N^{f,i}_{CaO} = \left(1 - \frac{\alpha^{f,i}}{100}\right) . N^{f,i-1}_{CaCO_3} + N^{f,i-1}_{CaO} \quad (4)$$

2.2.2 Macro- scale calculations

Based on elemental balances for the thermal decomposition of the sorbent, the conversion for $MgCO_3$ is expressed as:

$$\%\alpha_{MgCO_3}^{TD_i} = 100 \cdot \left(\frac{\Delta N_{CO_2}}{N_{MgCO_3}}\right) \qquad \text{for } \frac{\Delta N_{CO_2}}{N_{MgCO_3}} < 1, \tag{5}$$

and

$$\%\alpha_{MgCO_3}^{TD_i} = 100 \cdot \left(\frac{\Delta N_{CO_2} - N_{MgCO_3}}{N_{MgCO_3}}\right) \qquad \text{for } \frac{\Delta N_{CO_2}}{N_{MgCO_3}} \geq 1. \tag{6}$$

where ΔN_{CO_2} is the net number of CO_2 moles that have evolved from the reactor during the i^{th} thermal decomposition (TD_i) step, and N_{MgCO3} is the number of $MgCO_3$ moles in the 'fresh' dolomite.

The conversion (% $\alpha_{CaCO_3}^{i}$) for the calcination of $CaCO_3$, is,

$$\alpha_{CaCO_3}^{i}(\%) = 100 \cdot \frac{(\Delta N_{CO_2})}{N_{CaCO_3}^{f,i-1}} \qquad \text{for i>1 and } (-1)^i < 0. \tag{7}$$

ΔN_{CO_2} is given by integrating the number of moles dN_{CO_2} that are evolved in the reactor over a time interval *dt*, which in this case was every 5 s,

$$\Delta N_{CO_2} = \int_{t_0}^{t} dN_{CO_2} = \int_{t_0}^{t} x_{CO_{2,out}} \cdot \dot{N}_{dry,out} dt \tag{8}$$

For the carbonation steps the following equation for $(-1)^i > 0$, was used for the calculation of the molar conversion (% α_{CaO}^{i}),

$$\alpha_{CaO}^{i}(\%) = 100 \cdot \frac{(\Delta N_{CO_2})}{N_{CaO}^{f,i-1}} \tag{9}$$

The number of CO_2 moles consumed, ΔN_{CO_2} , was calculated by the following integral,

$$\Delta N_{CO_2} = \int_{t_0}^{t} dN_{CO_2} = \int_{t_0}^{t} (\dot{N}_{CO_{2,in}} - x_{CO_2,out} \cdot \dot{N}_{dry,out}) dt \quad (10)$$

3. Modelling theory

Useful kinetics for modelling purposes include the determination of the activation energy (E) and the reaction order (n) for the studied reactions. For this reason, the effects of temperature and gas concentration on the selected data were considered.

The improved iterative version of Coats- Redfern method (Urbanovici *et al.* 1999) was applied to evaluate the non- isothermal kinetic parameters. This method includes an iterative procedure which transforms the evaluation of the kinetic parameters (E and A (pre-exponential factor)) from a linear regression analysis. Additionally, the F- test (based on $F - ratio = S_{reg}/{S_{xy}}^2$, where S_{xy} : the sum of the squares of residual terms) was used as a complementary statistical criterion to identify the most probable mechanism function ($g(\alpha)$). Residual mean square ${S_{xy}}^2$ alone, cannot be used as a statistical criterion for selecting the most probable mechanism function, $g(\alpha)$, as suggested by Vyazovkin Lesnikovich (1986).

Reaction equations can potentially give the best simulation ('fit') of the experimental conversions as a temperature function for both micro- and macro- scale calcinations and carbonations based on the iterations' best correlation coefficient (r) and E as well as on the calculated *n* when the *n*th order reaction model is applied. The use of the F- test in the improved iterative Coats- Redfern method (Urbanovici *et al.* 1999) decreased the number of the considered kinetic to the following:

(1) the Jander (3D) diffusion model, $g(\alpha) = [1 - (1 - \alpha)^{\frac{1}{3}}]^2$

(2) the power law, $g(\alpha) = \alpha^{\frac{1}{m}}$, for m= 1,2,3 and 4

(3) the nth order reaction, $g(\alpha) = \frac{[1-(1-\alpha)^{1-n}]}{1-n}$ for n=1, $g(\alpha) = -\ln(1 - \alpha)$.

The Jander model works for solid state processes, which are limited by the diffusion of one of the components through a layer of the product (Jander 1927) and therefore belong to the group of diffusion-limited models. The Jander model is often referred to as being 3D because it is a combination of the parabolic law (1D) and the contracting volume equation for $n = 3$. The Jander (3D) diffusion mechanism is well established in describing the kinetics and reaction mechanisms in gas – solid systems, such as hydrogen adsorption, especially for storage materials (Dou *et al.* 2010, Cui *et al.* 2008).

The conversion curves of thermal decompositions in both 'dry' and 'wet' macro-scale experiments were normalized between 0 and 1 as the minimum and maximum points during this reaction. The normalized conversion fractions ($\alpha_{normalized}$) are calculated by the following equation:

$$\alpha_{normalized} = \frac{\Delta N_{CO_2,t=0} - \Delta N_{CO_{2,t}}}{\Delta N_{CO_2,t=0} - \Delta N_{CO_2,t,end}}$$

Uncertainties were considered based on an assumed error of 1% on both absolute temperature and conversion.

4. Results and discussion

4.1 Micro- scale

All calcinations were best described by the n^{th} order reaction equation and those following the first carbonations under 5 kPa CO_2 were of order 1.3 (Table 1). The calcinations following the first carbonation steps were harder to initiate compared to the earlier calcination steps as evidenced by the apparent calculated activation energies. The activation energies of the 2nd calcination which followed the 1st carbonation under all

conditions were higher in value. The larger presence of $CaCO_3$ in the sorbent, as indicated by the final conversions, reached in the 1st carbonation, might have delayed the initiation of the subsequent calcinations.

In the present study, diffusion was the governing kinetic control in the carbonation steps. In particular, the employment of the Jander (3D) integral kinetic equation which described the path of the reaction mechanism was employed and from the calculated kinetic parameters it was found that the conversion curves and the TGA data coincided. Hyatt *et al.* (1958) previously observed that the diffusion of CO_2 through $CaCO_3$ layers during re-carbonation might occur. Beruto *et al.* (1984) supported that the diffusion of CO_2 through the carbonate product layer on the surface of micropores was restricted by grain boundary layer diffusion. Additionally, it has been suggested that the CO_2 capture performance of Ca- based sorbents is enhanced by improving the diffusion of CO_2 through the product layer (Yi *et al.* 2009). Other researchers suggested that incomplete carbonations occurred due to the fact that the CO_2 reacted close to the exterior surface of a CaO particle, not allowing CO_2 to reach any CaO molecules closer to the particle centre (Chrissafis *et al.* 2005b). Therefore, the thicker the product ($CaCO_3$) layer grew, the slower the reaction became. It was observed that during all 2nd carbonations, higher activation energies were required. This could accentuate diffusion limited conditions in the reactive system which was further depicted in the final conversions reached (Table 2). Interestingly enough, at the 15 kPa carbonation, the required activation energy in both the 1st and 2nd carbonations was set in the lowest value scale, compared to those at 5 kPa and 10 kPa CO_2. In previous works (Sun *et al.* 2008) much lower values of the carbonation at 5 kPa CO_2 were calculated (26 kJ mol^{-1}) compared to this study (90.4 kJ mol^{-1}). This might be due to the fact that the apparent carbonation activation energy in that earlier work was produced by using the power law kinetic equation (Sun *et al.* 2008) when the present one was based on the Jander (3D) diffusion equation, resulting in more than twice as

large values between the first and second mechanism. Additionally, Urbanovici *et al.* (1999) found that a ratio of 2.7 was obtained in the case of isothermal $Mg(OH)_2$ dehydration when the power law equation was used compared to the Jander (3D) diffusion equation.

4.2 Macro- scale

No calcinations at macro- scale reached completion (α<<1), either under 'dry' or 'wet' conditions (Tables 2 and 3), during the heating up step as shown in the micro-scale study (Table 1). Still, the maximum conversion at macro-scale 'dry' conditions seemed to be affected in a positive way by the completeness of the previous carbonation All calcination steps were set to reach 800^{o}C in all experimental set- ups, since this is the maximum temperature employed in the air feed step corresponding to oxygen carrier regeneration (Dupont *et al.* 2007, Pimenidou *et al.* 2010a, Pimenidou et al. 2010b, Giannakeas *et al.* 2012, Dou *et al.* 2010). Actually, when switching from the air feed step to the fuel feed step, the temperature decreases from 800^{o}C to 600^{o}C, and based on the current experimental conversions' results it was noticed that calcination still took place. Due to the packing effect the sorbent's bed temperature reached temperatures higher than 800^{o}C. Calcination steps under 'dry' and 'wet' conditions concluded during the cooling down intervals possibly as a result of the heat accumulated within the sorbent's bed which allowed the further thermal decomposition of the material. This is the reason the experimental initial, maximum and final calcination temperatures for the 'dry' and 'wet' macro- scales in Table 2 are shown.

Despite that calcination steps were performed in an inert environment, a discontinuity in CO_2 released during these experiments occurred at the same temperature as that observed in the thermal stability 'dry' micro- scale calcination which occurred in the presence of CO_2. This could have occurred due to self-creation of a CO_2 atmosphere which resulted from the

larger mass of the sorbent used in the reactor. Such conditions were described by Bandi and Krapf (1976) and were attributed to the effect of the packing of the material. The presence of fines in both samples indicated the evolution of CO_2 during both 'dry' and 'wet' thermal decompositions and resulted in the breaking down of the dolomite particles, or the presence of any grains could have been an effect of calcination which produces more cracked grains as the sorbent decomposes (Figure 1). In previous studies (Silaban *et al.* 1996) it was noticed that the thermal decomposition in pure N_2 results in a more developed morphology, whereas in the presence of CO_2 (100 kPa CO_2) (Manovic *et al.* 2009) larger grains are developed as larger pore diameters are formed.

The apparent activation energies for the first 'dry' calcinations showed that these reactions were harder to initiate than under 'wet' conditions. Due to the non- isothermal conditions, once the temperatures for the initiation of $CaCO_3$ thermal decomposition in the sorbent bed were reached, the thermal decomposition of $MgCO_3$ was terminated. All calcinations were expressed by the reaction order model but with a different order value (Tables 1, 3 and 4). Olszak- Humienik and Możejko (1999) reported activation energies of 219 kJ mol^{-1} for the $MgCO_3$ thermal decomposition when using the Coats- Redfern method based on the diffusion (1D) equation. In that work, the calcination of $CaCO_3$ was expressed by the random nucleation model resulting in E= 390 kJ mol^{-1}. The latter value is in agreement with that of the 2nd 'dry' calcination following carbonation at 15 kPa CO_2.

All first 'dry' carbonations steps showed that the higher the partial pressure of CO_2 was, the lower the final values of conversions reached were. These results do not agree with those of the micro- scale study. Packing of the sorbent in the case of the macro- scale set- up might not allow enough reaction time of the CO_2 with the dolomite particles. The conversion reached by the end of the second carbonation for the middle CO_2 partial pressure (10 kPa)

exhibited the higher drop in value from the respective one in the first carbonation and when compared to the final conversions of the second carbonation steps at 5 and 15 kPa of CO_2.

Similarly to the present 'dry' macro- scale final carbonation conversions, Sun *et al.* (2008) noticed a better performance of carbonations when partial pressures of CO_2 smaller than 10 kPa were used, whereas for P_{CO_2} >10 kPa the respective performance was limited.

Experimental 'dry' carbonation conversions were extremely well reproduced from the iterative method described earlier based on the hypothesis of the Jander (3D) diffusion equation. The highest activation energy among the 1st carbonation steps was calculated at the lowest CO_2 partial pressure (5 kPa). This could be attributed to the extent of the preceding calcination ($\alpha \cong 0.84$) which was limited compared to those that preceded the first carbonations at 10 and 15 kPa CO_2 ($\alpha = 0.96$ and 0.91 respectively). Higher energy was needed during the second 'dry' carbonation at 10 kPa compared to the respective steps in the other two CO_2 conditions. During the second 'dry' carbonation at 15 kPa CO_2 the lowest final conversion for that step was attained which reflected on low apparent activation energies (i.e. 119 kJ mol^{-1}; Table 4).

The calculated conversion curves corresponding to the 1st carbonation are superimposable on the experimental curve for the whole range of conversions (Figure 2), while the correlation coefficients indicate an excellent model (Table 3).

4.2.1 The effect of steam

The final conversions of the sorbent's first calcination (e.g. 0.89 in the lower 'wet' CO_2 pressure regime) were not seriously affected by the use of steam when compared to the respective 'dry' macro- scale results (e.g. 0.84 at 5 kPa CO_2) (Table 2). Still the 2nd calcination at low partial pressures of steam resulted in an enhanced final conversion during

thermal decomposition (e.g. 2.8-6.8 kPa), but the effect was soon reversed at higher steam partial pressures (10.1 kPa). In past studies such as in McIntosh *et al.* (1990), the effect of steam appeared to have an enhancing impact on the thermal decomposition of Ca sorbents but not to the extent achieved in the present macro- scale study, especially at higher pressure regimes (Table 2). Higher final conversions were reached during the carbonations which might have been assisted by the presence of MgO, which resulted from the initial calcination of dolomite. The mobility of the CO_2 produced on the particles' surface might have been enhanced by the presence of steam resulting in a smaller residence time of the CO_2 produced than under 'dry' calcinations.

The calcinations' experimental conversions were best expressed by the reaction order model. The calculated reaction order was in the same value range in both the 'dry' and 'wet' 2^{nd} calcinations following the carbonation in the middle CO_2 concentration range (i.e. 10 kPa CO_2). Both 'dry' and 'wet' calculated activation energies for these 2^{nd} 'dry' and 'wet' calcinations were in the range of 300 kJ mol^{-1}. The 1^{st} 'wet' calcination at 15 kPa CO_2 was found to be of order 2.9, when the *n* for the 2^{nd} calcination was calculated to be equal to 1.2. The 2^{nd} 'wet' calcination at 15 kPa CO_2 was easier to initiate as evidenced by the calculated activation energies, than the respective 'dry' one. Due to the greater number of available $CaCO_3$ moles, as indicated by the final conversion reached (Table 2), on the outer layers of the surface of the sorbent particles present in the reactor, a smaller energy supply was necessary for their thermal decomposition. This is the most probable explanation rather than the presence of steam, which did not seem to affect the rest of the 2^{nd} 'wet' calcinations as shown in Tables 2 and 3.

The thermal swing regeneration step of the sorbent used in chemical looping reforming process may therefore benefit from the presence of a little steam but too much may prove counterproductive, and thus the safer approach would be to maintain 'dry' conditions

for calcination if possible. This is unlike hydrotalcite sorbents whose regeneration, under the thermal swing generated by steam addition, is recommended.

The 'wet' macro- scale experiments achieved a measurable positive effect on the final experimental absolute CO_2 capacity of the sorbent by increasing the carbonation reaction rate and the final conversions. The first and second carbonation curves in 'wet' conditions exhibited a greater activity than their 'dry macro and micro' counterparts (Figure 2). More specifically, the strongest effect of steam, promoting both the 1st and 2nd carbonations, was at the lowest and highest 'wet' CO_2 pressure regimes, while the effect of steam was slightly less for the middle 'wet' CO_2 pressure range. Steam could have resulted in a higher flow of the total gases and the better transport of CO_2 to the available CaO sites. For the lowest P_{CO_2}, the first 'wet' carbonation started at a lower temperature than the 'dry' one. It is worth noting that the temperatures where the carbonations began in this study were significantly lower than those reported in the literature (Abanades *et al.* 2007, Chrissafis *et al.* 2005a). This could be attributed to the non-isothermal conditions of the experiments, which allowed for the kinetic data generation from ambient to high temperatures, as opposed to the kinetic studies so far carried out at high temperature isothermal conditions.

The beneficial effect of steam at high CO_2 pressures was evidenced as carbonations were allowed to reach completeness (Table 2) based on the available CaO moles from the previous step. The catalytic presence of steam might have activated more sites during the carbonation steps which then led to a higher energy demand to reach the higher conversions at the higher 'wet' range of CO_2 pressures.

The kinetic parameters emerging from the micro- and macro- scale carbonation experiments are directly comparable since both were best calculated by the Jander (3D) diffusion equation. Any increase in the activation energies in the 'dry' and 'wet' macro- scale runs compared to those at 'dry' micro- scale is an issue that needs to be considered as it

clearly indicates that at macro- scale more energy is required to initiate carbonations. This might have to do with the larger masses employed and the packing of the material, as discussed earlier, as opposed to micro- scale and despite that in both cases the same size particles were used.

4.3 Thermal stability study

In neither the initial 'dry' nor 'wet' macro- scale thermal stability calcinations the sorbent was fully decomposed. The use of CO_2 and the additional CO_2 produced calcination might have retarded the extent of the decomposition of $MgCa(CO_3)_2$ into MgO.CaO (Figure 3a). In the past, it was found that the rate of calcination of the $CaCO_3$ could slow down the overall rate of the dolomite decomposition rather than the $MgCO_3$ decomposition (Otsuka *et al.* 1986). Furthermore, non-uniform temperature gradients among the mass of the sorbent might have contributed to the incomplete $MgCO_3$ and $CaCO_3$ thermal decompositions due to the material's packing and consequently the retention of additional CO_2 around the sorbent's particles. The same trend of incomplete calcinations was followed by all 8 calcinations that succeeded the 9 carbonations, contrary to the micro- scale thermal stability study (Figure 3a).

Two CO_2 peaks during the macro- scale thermal decompositions, which originated from the $MgCO_3$ and $CaCO_3$ decompositions respectively, were distinguished (Figure 4a). It was noticed that the CaO carbonation reaction concluded at temperatures close to the initialization temperatures of the $MgCO_3$ thermal decomposition. These temperatures were confirmed by the earlier determined micro- scale experiments (Figure 4b). In particular, the 'dry' thermal decomposition of $MgCO_3$ in the TGA at 10 kPa CO_2, occurred between 643 and 772°C while the 1st calcination of $CaCO_3$ started at 782°C and ended at 828°C. In the 'wet' experiments, the initial temperature of the $MgCO_3$ decomposition was lower than the

one under ‘dry’ conditions (587°C) whereas for the $CaCO_3$ the onset calcination temperature was in the range of 727-827°C.

Over the repeated calcination steps, these two CO_2 peaks tended to merge, forming a single curve with a shallow concavity, which was used to identify the temperature intervals of the two thermal decomposition reactions of $MgCO_3$ and $CaCO_3$. The formation and decomposition temperatures of salts at different CO_2 pressures have already been found, in the literature, to coincide at the temperatures at which the equilibrium pressure is the CO_2 pressure used in the experiment Criado and Dianez (2004). Based on the previous observations, $MgCO_3$ had completely converted into MgO by the 3rd cycle of the ‘dry’ macro- scale experiments, whereas when in the ‘wet’ ones, this was achieved by the 2nd cycle (Figure 3a). From the same figure it became evident that the presence of steam improved the final experimental conversions reached. Beruto *et al.* (2003) mentioned that steam would accelerate the rate of the first half of the thermal decomposition of dolomite, corresponding to the decomposition of $MgCO_3$, which is in agreement with this study. Moreover, the flow of steam could have allowed less residence time of the supplied and produced CO_2 compared to the ‘dry’ runs, something that promoted the thermal decomposition of $MgCO_3$. When natural dolomite is employed on a grams- scale in chemical looping reforming it should preferably be used in a fully decomposed form in order to avoid the incompleteness of the $MgCO_3$ calcination in order for the $CaCO_3$ formed during the fuel feed step to benefit from the rapid highly exothermic air feed step (Pimenidou *et al.* 2010b).

An expected decreasing trend of re- carbonation was observed over the repeated cycles, as seen earlier in the ‘dry’ micro- scale stability runs. Still, the ‘dry’ macro- scale carbonations from the 3rd till the 5th cycle performed better than the respective ones at micro-scale. The ‘dry’ macro- scale carbonations showed a sudden decrease in yield from the 6th to the 9th cycle, an effect that did not coincide with the micro- scale findings (Figure 3b). Even

though $MgCO_3$ was fully decomposed by the 2nd cycle under ‘wet’ conditions, the presence of MgO did not prevent sintering and the slow calcination can be attributed to shrunk or blocked passages as opposed to the expected high pore volume of the sorbent’s particles. In Figures 5a and 5b, the surface of the sorbent after the 9th carbonation at two magnifications (100 μm and 20 μm) might not be of high resolution but sintering was obvious even in the smaller magnification. Additionally, in the previous figures the MgO.CaO- $CaCO_3$ particles seemed solid and compact as a result of sintering, which limited any further carbonation. Similarly Chrissafis *et al.* (2005a) mentioned that sintering could limit the CaO carbonation over repeated cycles since there could not be sufficient diffusion of CO_2 through the CaO pores.

In the ‘dry’ macro- scale set- up, the final experimental conversions achieved in early carbonations were greater than the respective ‘wet’ ones. After the completion of the ‘dry’ decomposition of $MgCO_3$ which would no longer compete with the carbonation at the low temperature range during the 3rd, 4th and 5th carbonations, the values of the carbonation conversions were higher than in the first and second ones regardless of the extent of the $CaCO_3$ calcinations, and hence the higher availability of CaO at the beginning of the carbonation steps. This phenomenon was not noticed under the ‘wet’ conditions even when the $MgCO_3$ was fully decomposed. Additionally, under ‘wet’ conditions, the carbonation efficiency was more stable from cycle to cycle despite achieving lower conversions for up to the 8th cycle compared to the ‘dry’ carbonations from cycle 1 to 8 (Figure 3b). A similar effect of steam under chemical looping reforming conditions was evidenced by Pimenidou *et al.* (2010b) where the extent of CaO carbonation was stable from cycle 2 to 6. In Figure 3b it can be seen that by the ‘dry’ 9th carbonation the conversion fraction was poorer than under the ‘wet’ conditions. Therefore, despite the lower performance of the ‘wet’ carbonations over

the ‘dry’ ones, the presence of steam actually enhanced the stability of the sorbent over the 9 cycles in terms of CO_2 adsorption.

The repeated cycles of calcination/ carbonation exhibited an asymptotic trend in CO_2 capture performance which could be due to the equilibrium reached between the reduction of the surface area and pore volume (Florin and Harris 2009). In theory, highly sintered dolomite could be a suitable sorbent for SO_2 removal because of the regeneration of macro-pores during the calcination/ carbonation cycles (Sun *et al.* 2007). When sulphur containing fuels are used, lower effective diffusivity will characterize the CaO based sorbent. Sintering decreases the number of small pores and creates large ones which can accelerate calcination in later stages which enhances SO_2 capture.

5. Conclusions

This study has demonstrated the effect of sample weight, set- up (scale) and steam on the CO_2 capture performance of naturally formed dolomite under conditions imitating those of chemical looping steam reforming. The lab reactor scale indicated that a self- evolving atmosphere of CO_2 during the calcination steps (i.e. regeneration of sorbent) could reduce the extent of production of the desired CaO amount of capturing CO_2 in the carbonation steps (i.e. in steam reforming). Steam appeared to have a positive effect on CO_2 capture at its highest employed pressure regime (i.e. 15 kPa CO_2/ 10.1 kPa H_2O).

The carbonation reactions were diffusion limited at all scales and conditions (‘dry’ and ‘wet’), which was evidenced by the shape of the experimental conversion curves and the equation (Jander (3D)) used to reproduce the modelled conversion curves. The calculated activation energies at the highest ‘dry’ pressure regime of CO_2 at larger scale confirmed that the presence of steam had a positive catalytic effect on the sorbent’s final conversions.

Therefore, the use of in- situ CO_2 capture should promote fast kinetics and the CO_2 chemisorption in delivering high H_2 purity, enhance fuel conversion, and lower operational temperatures, better than in the absence of sorbent.

The thermal stability study at both tested scales under all conditions indicated large decay of the sorbent's capture in CO_2 due to sintering of the material. Still, the presence of steam exhibited a stabilisation effect on the sorbents carbonation conversions at the final larger scale cycles.

Overall, the present study showed that the in- situ use of naturally formed dolomite for chemical looping steam reforming could benefit from the absence of steam during the regeneration steps of the sorbent. Full calcination of the sorbent shouldn't be expected as indicated by the present larger scale study and compared to the present and earlier milli- gram scale investigations. On the other hand, the higher CO_2 partial pressures created during the steam reforming steps and the 'wet' conditions are expected to boost the sorbent's CO_2 capture efficiency despite the expected natural decay due to sintering which over repeated cycles should be stabilised.

Acknowledgements

Our thanks to James Wylie from WBB minerals for providing the dolomite (Warmsworth quarry, UK).

Funding

We would like to acknowledge the UK's Engineering and Physical Sciences Research Council for the EP/D078199/1 grant: 'Unmixed steam reforming of liquid fuels from biomass and waste for hydrogen production'.

References

Abanades, J. C. and Alvarez, D., 2003. Conversion limits in the reaction of CO_2 with lime. *Energy and Fuels*, 17, 308-315.

Abanades J.C. *et al.*, 2007. Cost structure of a Postcombustion CO_2 capture system using CaO. *Enviromental Science and Technology*, 41, 5523–5527.

Aihara M. T. Nagai, J. Matsushita,Y. Negishi, and H. Ohya. 2001. Development of porous solid reactant for thermal-energy storage and temperature upgrade using carbonation/ decarbonation reaction. *Applied Energ*y, 69, 225-238.

Bandi, W. and Krapf, G., 1976. The effect of CO_2 pressure and alkali salt on the mechanism of decomposition of dolomite. *Thermochimica Acta*, 14, 221-243.

Barker R., 1973. The reversibility of the reaction $CaCO_3 \rightleftarrows CaO+CO_2$. *Journal of Applied Chemistry and Biotechnology*, 23, 711- 779.

Beruto D., Barco L. and Searcy A.W., 1984. CO_2-Catalyzed Surface Area and Porosity Changes in High-Surface-Area CaO Aggregates. *Journal of American Ceramic Society*, 67, 512-515.

Beruto D. T., Vecchiattini R. and Giordani M., 2003. Effects of mixtures of H_2O (g) and CO_2 (g) on the thermal half decomposition of dolomite natural stone in high CO_2 pressure regime. *Thermochimica Acta*, 404, 25-33.

Blamey J., E. J. Anthony, J. Wang, and P. S. Fennell. 2010. The calcium looping cycle for large-scale CO_2 capture. *Progress in Energy and Combustion*, 36, 260-279.

Chen Z., Grace J. R. and Lim C. J, 2011. CO_2 capture and hydrogen production in an integrated fluidized bed reformer- regenerator system. *Industrial and Engineering Chemistry Research*, 50, 4716- 4721.

Chrissafis K., Dagounaki C. and Paraskevopoulos K. M., 2005a. The effect of sintering on the maximum capture efficiency of CO_2 using a carbonation/calcination cycle of carbonate rocks. *Journal of Thermal Analysis Calorim*etry, 81, 463- 468.

Chrissafis K., Dagounaki C. and Paraskevopoulos K. M., 2005b. The effects of the procedural variables on the maximum capture efficiency of CO_2 using a carbonation/ calcination cycle of carbonate rocks. *Thermochimica Acta*, 428, 193-198.

Criado J. M. and Dianez M.J., 2004. Influence on the mechanical treatment on the structure and the thermal stability of alkaline- earth carbonates. *Journal of Material Sci*ence, 39, 5189- 5193.

Cui X.Y. *et al.*, 2008. Comparative study on the hydriding kinetics of Zr-based AB_2 hydrogen storage alloys. *Intermetallics*, 16, 662- 667.

Curran G.P., Fink C. and Gorin E. 1967. The CO_2 acceptor gasification process. *American Chemical Society, Division* of *Fuel Chemistry,* 8, 128- 146.

Ding Y. and Alpay E., 2000. Equilibria and kinetics of CO_2 adsorption on hydrotalcite adsorbent. *Chemical Engineering Science*, 55, 3461-3474.

Dou B., G. L. Rickett,V. Dupont, P.T.Williams, H. Chen,Y. Ding, and M. Ghadiri. 2010. Steam reforming of crude glycerol with in situ CO_2 sorption. *Bioresource Technol*ogy, 101, 2436-2442.

Dupont V., A. B. Ross, I. Hanley, and M. V. Twigg. 2007. Unmixed steam reforming of methane and sunflower oil: A single-reactor process for H_2-rich gas. *International Journal of Hydrogen Energy,* 32, 67-69.

Ficicilar B. and Dogu T. 2006. Breakthrough analysis for CO_2 removal by activated hydrotalcite and soda ash. *Catalysis Today***,** 115, 274-278.

Florin N.H. and Harris A.T., 2009. Reactivity of CaO derived from nano-sized $CaCO_3$ particles through multiple CO_2 capture-and-release cycles. *Chemical Engineering Science,* 64, 187-191.

Giannakeas N., A. Lea-Langton, V. Dupont, and M. V. Twigg.. 2012. Hydrogen from scrap tyre oil via steam reforming and chemical looping in a packed bed reactor. *Applied Catalysis. B: Environ*mental, 126, 249-257.

Gupta H. and Fan L.-S., 2002. Carbonation−Calcination Cycle Using High Reactivity Calcium Oxide for Carbon Dioxide Separation from Flue Gas. *Industrial and Engineering Chemistry Research,* 41, 4035–4042.

Han C. and Harrison D.P., 1994. Simultaneous shift reaction and carbon dioxide separation for the direct production of hydrogen. *Chemical Engineering Science,* 49, 5875-5883.

Hyatt E.P., Cutler I.B. and Wadsworth M.E., 1958. Calcium carbonate decomposition in carbon dioxide atmosphere. *Journal of American Chemical Society,* 41, 70- 74.

Jander W., 1927. Reaktionen im festen Zustandebei höheren Temperaturen. *Zeischrift für anorganische und allgemeine Chemie,* 168, 113- 124.

L'vov B.V. and Ugolkov V.L., 2003. Kinetics of free-surface decomposition of dolomite single crystals and powders analyzed thermogravimetrically by the third-law method. *Thermochimica Acta,* 401, 139-147.

Lee D. K., 2004. An apparent kinetic model for the carbonation of calcium oxide by carbon dioxide. *Chemical Engineering Journal,* 100, 71-77.

Li Y., C. Zhao, L. Duan, C. Liang, Q. Li, W. Zhou, and H. Chen. 2008. Cyclic calcination/carbonation looping of dolomite modified with acetic acid for CO_2 capture. *Fuel Processing Technology,* 89, 1461-1469.

Lyon R. K. and Cole J. A., 2000. Unmixed combustion: An alternative to fire. *Combustion and Flame.* 121, 249- 261.

Manovic V., Anthony E.J. and Loncarevic D., 2009. CO_2 looping cycles with CaO-based sorbent pretreated in CO_2 at high temperature. *Chemical Engineering Science,* 64, 3236-3245.

McIntosh R.M., Sharp J.H. and Wilburn F.W., 1990. The thermal decomposition of dolomite, *Thermochimica Acta*, 165, 281- 296.

Ochoa-Fernández E., C. Lacalle-Vila, T. Zhao, M. Ronning, and D. Chen. 2007. Experimental demonstration of H_2 production by CO_2 sorption enhanced steam methane reforming using ceramic acceptors. *Studies in Surface Science and Catalysis*, 167, 159-164.

Olszak-Humienik M. and Możejko J., 1999. Kinetics of thermal decomposition of dolomite. *Journal of Thermal Analysis Calorimetry*, 56, 829-833.

Otsuka K. and Nakajima T., 1986. Partial oxidation of methane over rare earth metal oxides using N_2O and O_2 as oxidants. *Inorganic Chimica Acta*, 120, L27-L28.

Pimenidou P., G. L. Rickett, V. Dupont, and M. V. Twigg. 2010a. Chemical looping reforming of waste cooking oil in packed bed reactor. *Bioresource Technology*, 101, 6389-6397.

Pimenidou P., G. L. Rickett, V. Dupont, and M. V. Twigg. 2010b. High purity H_2 by sorption- enhanced chemical looping reforming of waste cooking oil in a packed bed reactor. *Bioresource Technol*ogy, 101, 9279- 9286.

Rao, A. B. and Rubin E. S., 2006. A technical, economic and environmental assessment of amine based CO_2 capture technology for power plant greenhouse gas control. *Enviromental Science and Technology*, 36, 4467−4475.

Romeo L. M., Y. Lara, P. Lisbona, and A. Martinez. 2009. Economical assessment of competitive enhanced limestones for CO_2 capture cycles in power plants. *Fuel Processing Technology,* 90, 803- 811.

Samtani M., Dollimore D. and Alexander K.S., 2002. Comparison of dolomite decomposition kinetics with related carbonates and the effect of procedural variables on its kinetic parameters. *Thermochimica Acta,* 392- 393, 135- 145.

Silaban A., Narcida M. and Harrison D.P., 1996. Characteristics of the reversible reaction between $CO_{2(g)}$ and calcined dolomite. *Chemical Engineering Communications,* 146, 149-162.

Squires A.M., 1967. Cyclic use of calcined dolomite to desulfurize fuels undergoing gasification. *Advances in Chemistry Series,* 69**,** 205–229.

Sun P., J.R. Grace, C. J. Lim, and E. J. Anthony. 2007. Sequential capture of CO_2 and SO_2 in a pressurized TGA simulating FBC conditions. *Environmental Science and Technology,* 41, 2943-2949.

Sun P., J.R. Grace, C. J. Lim, and E. J. Anthony. 2008. Determination of intrinsic rate constants of the CaO–CO_2 reaction. *Chemical Engineering Science.* 63, 47-56

Urbanovici E., Popescu C. and Segal E., 1999. Improved iterative version of the Coats- Redfern method to evaluate non- isothermal kinetic parameters. *Journal of Thermal Analysis Calorimetry,* 58, 683- 700.

Vyazovkin S. V. Lesnikovich and A. I., 1986. Some aspects of mathematical statistics as applied to non-isothermal kinetics. *Journal of Thermal Analysis,* 31, 319- 324.

Yi K.B., C.H. Ko, J.H. Park, and J.N. Kim. 2009. Improvement of the cyclic stability of high temperature CO_2 absorbent by the addition of oxygen vacancy possessing material. *Catalysis Today,* 146 (1-2), 241-247.

(a)

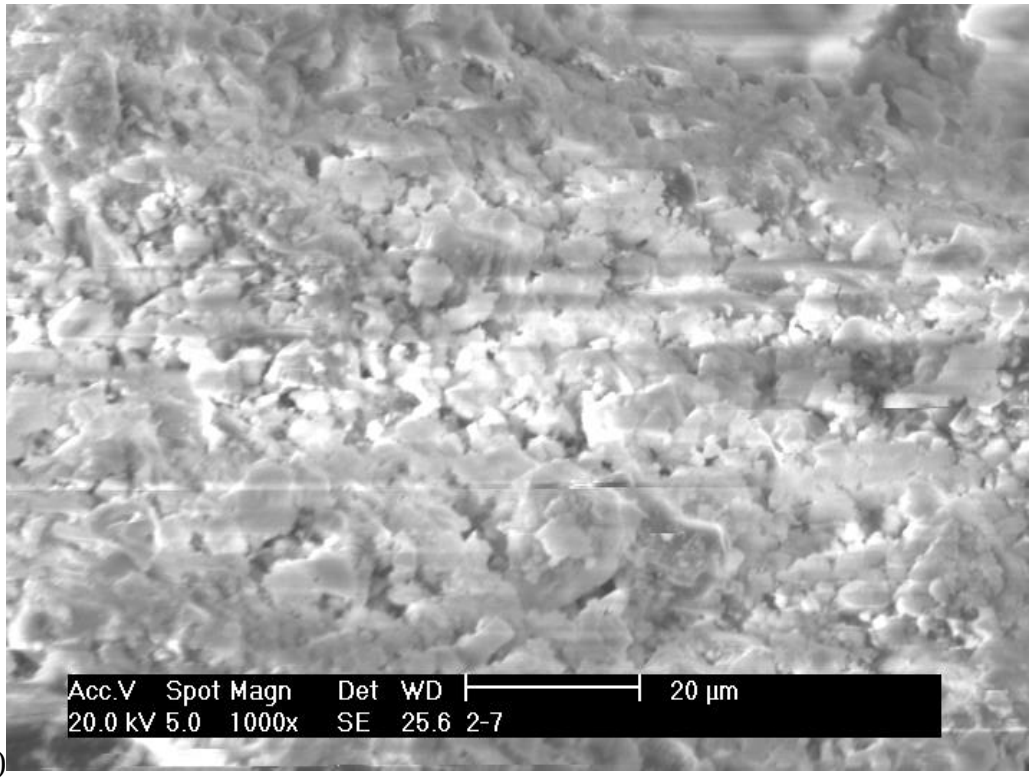

(b)

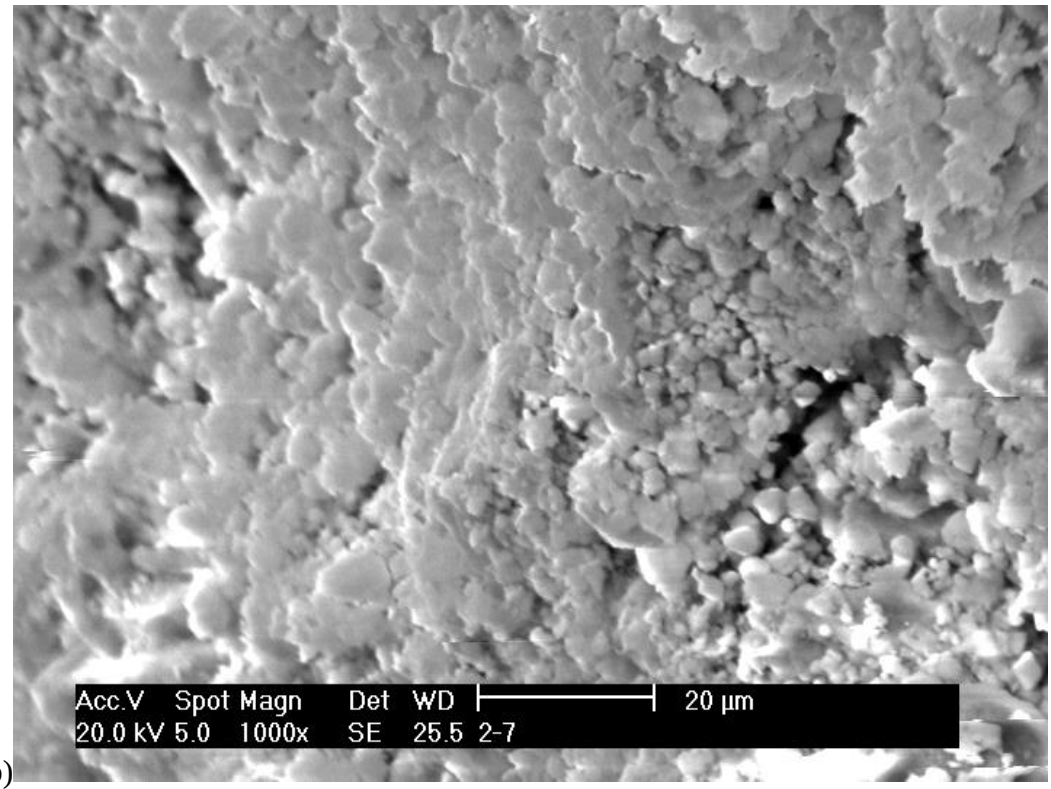

Figure 1. (a) 'Dry' and (b) 'wet' macro- scale SEM images of the sorbent after the 1st thermal decomposition at 100 kPa N_2.

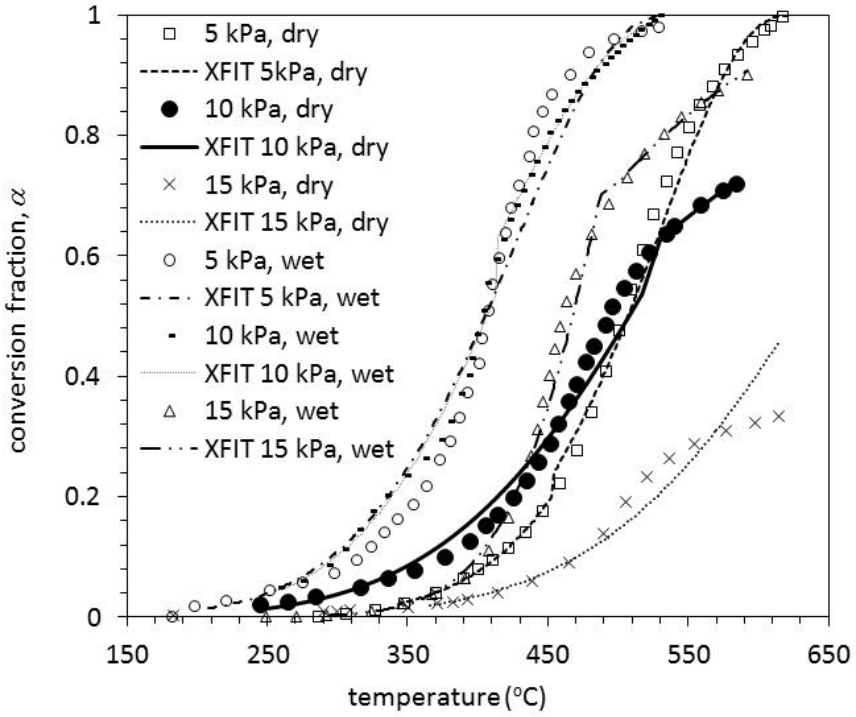

(a)

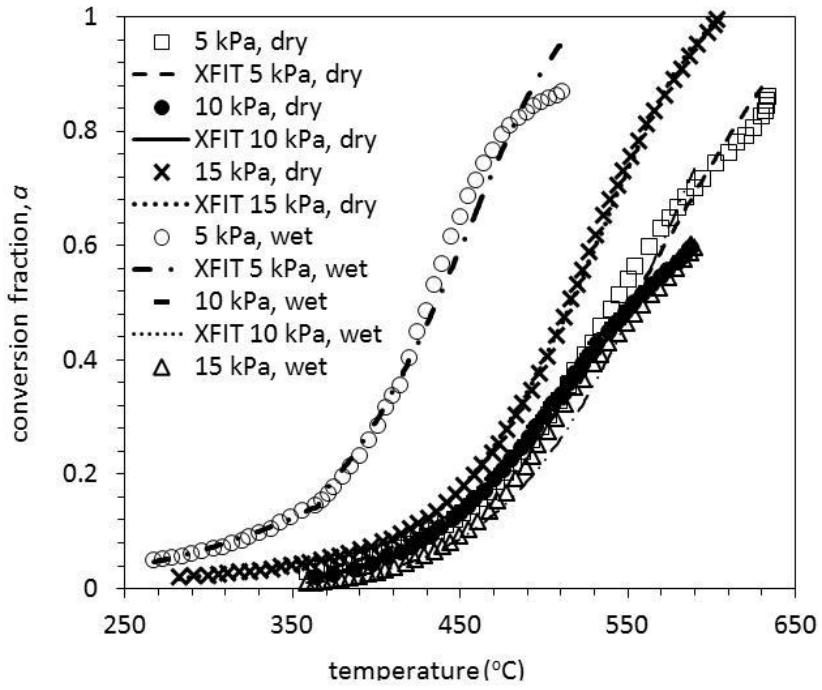

(b)

Figure 2. 'Dry' and 'wet' macro- scale experimental conversion (α) at and model fit (α_{FIT}) of the (a) 1st and (b) 2nd carbonations; at 5, 10 and 15 kPa CO_2 over temperature.

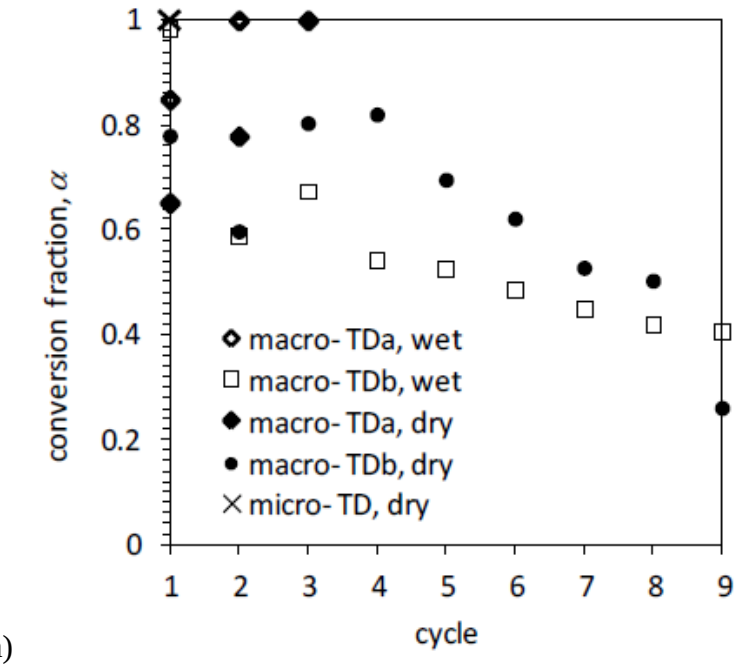

(a)

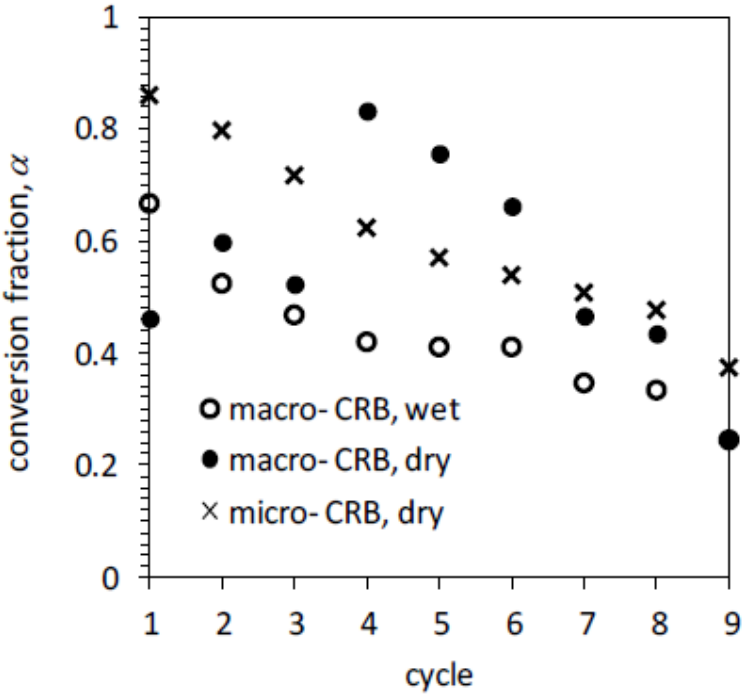

(b)

Figure 3. Micro- (‘dry’) and macro- scale (‘dry’ and ‘wet’) conversions of 9 consecutive (a) thermal decomposition- (b) carbonation cycles. Carbonations under ‘dry’ condition at 10 kPa CO_2 and under ‘wet’ conditions at 10 kPa CO_2/ 6.8 kPa H_2O.

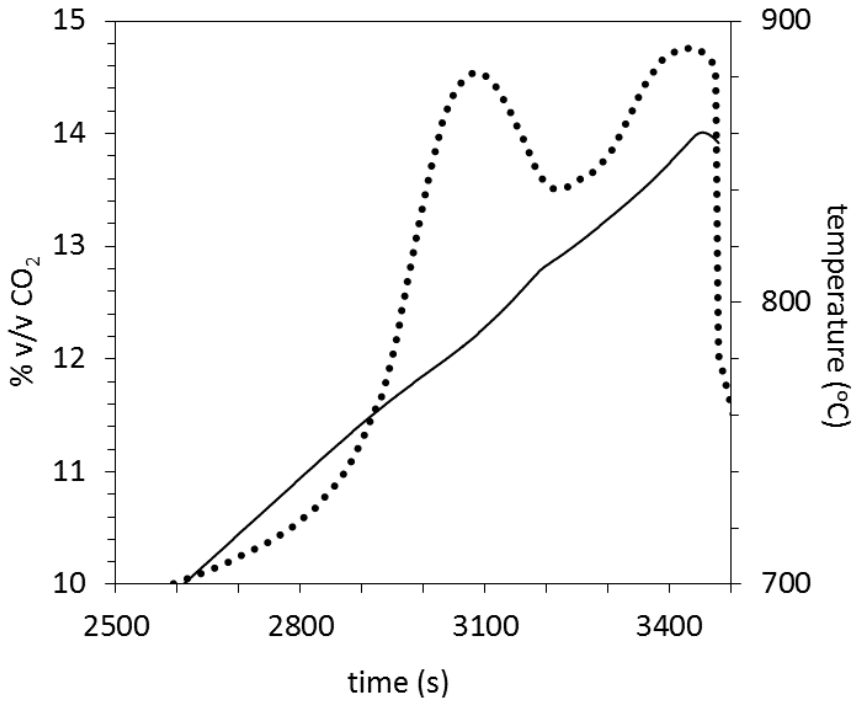

(a)

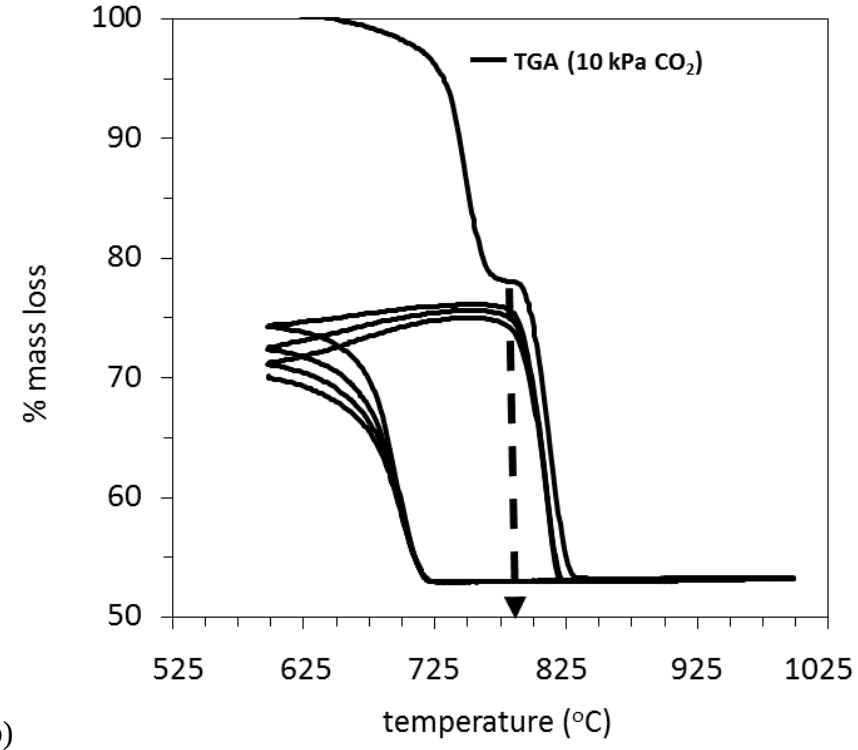

(b)

Figure 4. (a) CO_2 concentration (scatter points) and reactor temperature (line) with time. First peak corresponds to the $MgCO_3$ decomposition; second peak is the $CaCO_3$ decomposition in macro- scale ('dry') (b) micro- scale (same conditions) temperatures (the arrow indicates the initial temperature of the first thermal decomposition of $CaCO_3$).

(a)

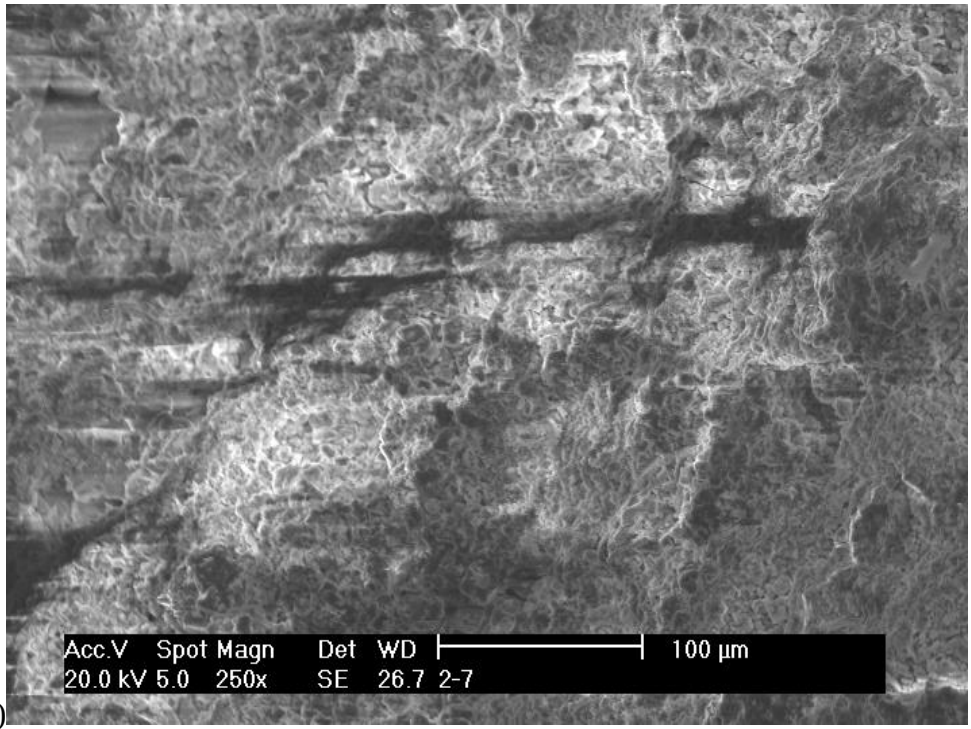

(b)

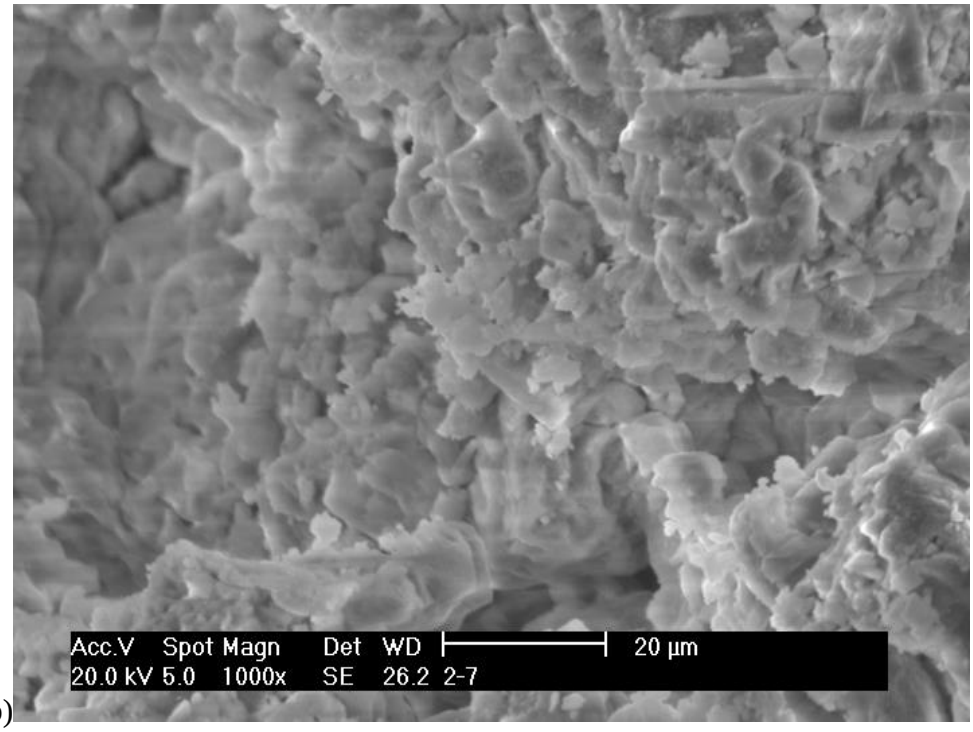

Figure 5. 'Wet' macro- scale SEM images of the sorbent after the 9th carbonation step at 10 kPa CO_2/ 6.8 kPa H_2O at (a) 250x and (b) 1000x magnification.

Table 1. Kinetic parameters for 'dry' carbonations at 5 kPa CO_2 at both micro- and macro- scales, 'wet' carbonations at 5 kPa CO_2/ 2.8 kPa H_2O at macro- scale and thermal decompositions ('dry' and 'wet') of the sorbent based on the reaction order model $g(\alpha) = \frac{[1-(1-\alpha)^{1-n}]}{1-n}$ and the Jander diffusion equation $g(\alpha) = [1-(1-\alpha)^{\frac{1}{3}}]^2$; correlation coefficient values (r) and conversions (α) of the applied model.

			1st carbonation					**2nd carbonation**				
scale	**Phase**	**model ($g(\alpha)$)**	**E±dE (kJ mol^{-1})**	**lnA±dlnA (A in s^{-1})**	***n***	***r***	**conv. fit**	**E±dE (kJ mol^{-1})**	**lnA±dlnA (A in s^{-1})**	***n***	***r***	**conv. fit**
micro- 'dry'	PH1	Jander (3D)	90.4±0.8	6.4±7.6	N/A	0.99	0.06-0.82	218±2	25.4±9	N/A	0.99	0.01-0.41
	PH2	Jander (3D)	Ø	Ø	N/A	Ø	Ø	31.1±0.8	-5.4±7	N/A	0.97	0.41-0.61
macro- 'dry'	PH1	Jander (3D)	144.6±-3.8	13.5±8.7	N/A	1	0.02-0.19	127.5±9.2	9.9±7.9	N/A	0.99	0.03-0.86
	PH2	Jander (3D)	141.0±-2.2	13.3±8.3	N/A	1	0.20-0.99	Ø	Ø	N/A	Ø	Ø
macro- 'wet'	PH1	Jander (3D)	94.7±-0.4	8.3±7.6	N/A	0.98	0.02-0.98	59.3±-2.2	-0.47±7.5	N/A	0.99	0.00-0.15
	PH2	Jander (3D)	Ø	Ø	N/A	Ø	Ø	128.4±-2.1	13.43±8.2	N/A	0.99	0.15-0.87
			1st thermal decomposition					**2nd thermal decomposition**				
scale	**Phase**	**model ($g(\alpha)$)**	**E±dE (kJ mol^{-1})**	**lnA±dlnA (A in s^{-1})**	***n***	***r***	**conv. fit**	**E±dE (kJ mol^{-1})**	**lnA±dlnA (A in s^{-1})**	***n***	***r***	**conv. fit**
micro- 'dry'	PH1	reac. ord.	880±37	102±5	1.3	0.99	0.03-0.9	900±96	107±12	1.3	0.99	0.02-0.98
	PH2	reac. ord.	Ø	Ø	Ø	Ø	Ø	Ø	Ø	Ø	Ø	Ø
macro- 'dry'	PH1	reac. ord.	1341.3±327.1	143.4±39.0	2.9	1	0.03-0.48	218.4±3.3	19.6±0.4	1.8	1	0.02-0.81
	PH2	reac. ord.	Ø	Ø	Ø	Ø	Ø	Ø	Ø	Ø	Ø	Ø
macro- 'wet'	PH1	reac. ord.	129.4±1	7.5±0.2	0	1	0.01- 0.6	257.0±4.2	23.7±0.5	1.8	1	0.02-0.83
	PH2	reac. ord.	Ø	Ø	Ø	Ø	0.02-0.83	Ø	Ø	Ø	Ø	Ø

Table 2. Final conversions (α) and temperature intervals for the carbonations/ thermal decompositions at 'dry' micro- and macro-scales and the 'wet' macro- scale set- up used for the calculation of kinetic parameters.

	1st carbonation 5 kPa CO_2- 5 kPa CO_2/ 2.8 kPa H_2O		**2nd carbonation**		**1st carbonation** 10 kPa CO_2/ 10 kPa CO_2- 6.8 kPa H_2O		**2nd carbonation**		**1st carbonation** 15 kPa CO_2/ 15 kPa CO_2- 10.1 kPa H_2O		**2nd carbonation**	
scale	**(α)**	**T_i-T_f (^{o}C)**	**(α)**	**T_i-T_f (^{o}C)**	**(α)**	**T_i-T_f (^{o}C)**	**(α)**	**T_i-T_f (^{o}C)**	**(α)**	**T_i-T_f (^{o}C)**	**(α)**	**T_i-T_f (^{o}C)**
micro- 'dry'	0.83	155-449	0.61	329-616	0.90	245-543	0.73	285-620	0.84	224-553	0.88	284-640
macro- 'dry'	1	308-656	0.88	302-636	0.72	132-601	0.60	312-588	0.33	160-615	0.26	190-604
macro- 'wet'	0.98	183-524	0.92	193-547	0.99	218-528	0.86	147-418	0.90	325-591	0.60	377-589
	1st thermal decomposition		**2nd thermal decomposition**		**1st thermal decomposition**		**2nd thermal decomposition**		**1st thermal decomposition**		**2nd thermal decomposition**	
scale	**(α)**	**T_i-T_f (^{o}C)**	**(α)**	**T_i-T_f (^{o}C)**	**(α)**	**T_i-T_f (^{o}C)**	**(α)**	**T_i-T_f (^{o}C)**	**(α)**	**T_i-T_f (^{o}C)**	**(α)**	**T_i-T_f (^{o}C)**
micro- 'dry'	1	705-750	1	690-713	1	724-777	1	685-736	1	717-768	1	626-719
macro- 'dry'	0.84	493-824-747	0.90	470-823-677	0.96	571-814-680	0.88	627-810	0.91	585-817-596	0.81	656-820
macro- 'wet'	0.89	577-827-667	0.97	695-829-667	0.89	523-877-657	0.85	693-751-686	0.89	638-861-491	0.64	675-877-695

Table 3. Kinetic parameters for 'dry' carbonations at 10 kPa CO_2 at both micro- and macro- scale, 'wet' carbonations at 10 kPa CO_2/ 6.8 kPa H_2O at macro- scale and thermal decompositions ('dry' and 'wet') of the sorbent based on the reaction order model $g(\alpha) = \frac{[1-(1-\alpha)^{1-n}]}{1-n}$ and the Jander diffusion equation $g(\alpha) = [1-(1-\alpha)^{\frac{1}{3}}]^2$; correlation coefficient values (r) and conversions (α) of the applied model.

			1st carbonation					**2nd carbonation**				
scale	**Phase**	**model ($g(\alpha)$)**	**E±dE (kJ mol^{-1})**	**lnA±dlnA (A in s^{-1})**	***n***	***r***	**conv. fit**	**E±dE (kJ mol^{-1})**	**lnA±dlnA (A in s^{-1})**	***n***	***r***	**conv. fit**
micro- 'dry'	PH1	Jander (3D)	115.1± -1.6	10.6±8.1	N/A	1	0.02-0.39	239.4± -5.5	29.1±9.4	N/A	0.99	0.02-0.43
	PH2	Jander (3D)	122.7± -6.1	12.1±8.8	N/A	0.99	0.41-0.82	40.0± -1.8	-3.6±6.9	N/A	0.99	0.44-0.73
macro- 'dry'	PH1	Jander (3D)	95.2±-0.7	6.0±7.7	N/A	0.99	0.03-0.72	160.8±-3.1	15.6±8.6	N/A	1	0.02-0.30
	PH2	Jander (3D)	Ø	Ø	N/A	Ø	Ø	89.7±-4.5	4.0±8.2	N/A	0.99	0.30-0.60
macro- 'wet'	PH1	Jander (3D)	97.6±-1.4	8.75±7.9	N/A	0.99	0.05-0.60	237.4±-1.9	29.89±8.8	N/A	0.99	0.01-0.82
	PH2	Jander (3D)	72.5±-2.2	4.50±7.7	N/A	1	0.06-1	Ø	Ø	N/A	Ø	Ø
			1st thermal decomposition					**2nd thermal decomposition**				
scale	**Phase**	**model ($g(\alpha)$)**	**E±dE (kJ mol^{-1})**	**lnA±dlnA (A in s^{-1})**	***n***	***r***	**conv. fit**	**E±dE (kJ mol^{-1})**	**lnA±dlnA (A in s^{-1})**	***n***	***r***	**conv. fit**
micro- 'dry'	PH1	reac. ord.	677.9±58.2	77.9±7.3	1.2	0.99	0.03-0.99	972.8±117.9	113.7±14.8	1.6	0.99	0.03-1
	PH2	reac. ord.	Ø	Ø	Ø	Ø	Ø	Ø	Ø	Ø	Ø	Ø
macro- 'dry'	PH1	reac. ord.	1064.8±134.0	115.6±15.6	1.2	0.99	0.03-0.99	318.9±6.0	32.7±0.73	2.6	1	0.03-0.84
	PH2	reac. ord.	Ø	Ø	Ø	Ø	(normalised)	Ø	Ø	Ø	Ø	Ø
macro- 'wet'	PH1	reac. ord.	99.54±1.68	3.30±-0.2	0	1	0.03-0.85	323.79±5.4	30.7±0.64	2.9	1	0.02-0.69
	PH2	reac. ord.	Ø	Ø	Ø	Ø	Ø	Ø	Ø	Ø	Ø	Ø

Table 4. Kinetic parameters for 'dry' carbonations at 15 kPa CO_2 at both micro- and macro- scales, 'wet' carbonations at 15 kPa CO_2/ 10.1 kPa H_2O at macro- scale and thermal decompositions ('dry' and 'wet') of the sorbent based on the reaction order model $g(\alpha) = \frac{[1-(1-\alpha)^{1-n}]}{1-n}$ and the Jander diffusion equation $g(\alpha) = [1-(1-\alpha)^{\frac{1}{3}}]^2$; correlation coefficient values (r) and conversions (α) of the applied model.

			1st carbonation					**2nd carbonation**				
scale	**Phase**	**model ($g(\alpha)$)**	**E±dE (kJ mol^{-1})**	**lnA±dlnA (A in s^{-1})**	***n***	***r***	**conv. fit**	**E±dE (kJ mol^{-1})**	**lnA±dlnA (A in s^{-1})**	***n***	***r***	**conv. fit**
micro- 'dry'	PH1	Jander (3D)	77.5± -2.5	3.5±7.8	N/A	0.99	0.07-0.25	103.9± -0.6	7.6±7.7	N/A	0.99	0.02-0.91
	PH2	Jander (3D)	142.1± -2.7	15.1±8.4	N/A	0.99	0.26-0.97	Ø	Ø	N/A	Ø	Ø
macro- 'dry'	PH1	Jander (3D)	135.7±-2.1	10.1±8.2	N/A	0.99	0.03-0.30	119.9±-0.9	6.5±7.9	N/A	0.99	0.01-0.26
	PH2	Jander (3D)	164.2±-16.7	9.4±7.8	N/A	0.99	0.31-0.34	Ø	Ø	N/A	Ø	Ø
macro- 'wet'	PH1	Jander (3D)	206.8±-1.96	25.6±8.7	N/A	1	0.03-0.7	175.1±-1.2	17.1±8.4	N/A	1	0.03-0.6
	PH2	Jander (3D)	43±-3.1	-1.7±7.2	N/A	0.99	0.7-0.9	Ø	Ø	N/A	Ø	Ø
			1st thermal decomposition					**2nd thermal decomposition**				
scale	**Phase**	**model ($g(\alpha)$)**	**E±dE (kJ mol^{-1})**	**lnA±dlnA (A in s^{-1})**	***n***	***r***	**conv. fit**	**E±dE (kJ mol^{-1})**	**lnA±dlnA (A in s^{-1})**	***n***	***r***	**conv. fit**
micro- 'dry'	PH1	reac. ord.	360.4±12.8	40±1.6	1.1	1	0.03-0.99	578.5±36.9	66.7±4.7	1.2	0.99	0.03-0.99
	PH2	reac. ord.	Ø	Ø	Ø	Ø	Ø	Ø	Ø	Ø	Ø	Ø
macro- 'dry'	PH1	reac. ord.	1269.7±207.0	138.5±24.2	1.7	0.99	0.04-0.97	412.1±7.6	43.8±0.9	1.5	0.99	0.03-0.99
	PH2	reac. ord.	Ø	Ø	Ø	Ø	(normalised)	Ø	Ø	Ø	Ø	(normalised)
macro- 'wet'	PH1	reac. ord.	975±841.2	99.9±235.4	2.9	0.99	0.06-0.19	239.2±4.1	21.7±0.5	1.2	0.99	0.03-1
	PH2	reac. ord.	563.7±242.3	54.9±32.3	2.4	1	0.20-0.40	Ø	Ø	Ø	Ø	(normalised)